the boundary conditon

$$[\partial J_m(\beta r)/\partial r]_{r=R}=0, \tag{3}$$

where $J_m(\beta r)$ is a Bessel function of order m. Assuming $c=10^5$ cm/sec and $R=5.2$ cm, the frequency associated with the lowest order radial mode is $f_{100}\approx 11.7$ kHz, and for the lowest order azimuthal mode is $f_{010}\approx 5.6$ kHz. Both of these values are in approximate agreement with the frequencies observed.

It is apparent that the oscillations are neither generated in the steady-state plasma nor in the observable afterglow. The generation of these oscillations must be associated with power turnoff. It is evident that expression (1) is not satisfied in the steady-state plasma; however, the possibility that it might be satisfied at power turnoff should be considered. If the cooling time for the neutral gas t_n is less than the cooling time for the electrons t_e, the quantity T_e/T_n might increase sufficiently at power turnoff to cause expression (1) to be satisfied. Assuming a weakly ionized plasma,

$$t_n\approx T_{nn} \text{ and } t_e\approx T_{en}/\epsilon,$$

where T_{nn} is the neutral-neutral collision time, T_{en} is the electron-neutral collision time, and ϵ is the fractional energy-transfer coefficient for electron-neutral collisions. At a pressure $p_g=0.1$ Torr, and assuming that $\epsilon=2m_e/(m_e+m_n)$, the cooling times at power turnoff are found to be

$$t_n\approx 10^{-6} \text{ and } t_e\approx 10^{-5} \text{ sec.}$$

Thus, an increase in T_e/T_n is possible at power turnoff. Such an increase, however, should be small, since T_n in the steady-state plasma is only slightly greater than its equilibrium value in the neutral gas. If expression (1) is close to being satisfied for the steady-state plasma, a small increase in T_e'/T_n, at power turnoff, may be sufficient to generate oscillations. Assuming $p_g=0.1$ Torr, the steady-state plasma parameters were estimated to be as follows:

$$N_e/N_n\approx 2\times 10^{-5}, \quad T_e/T_n\approx 180,$$

$$l_e\approx 0.5 \text{ cm}, \quad l_n\approx 0.1 \text{ cm}.$$

Substituting these parameters into the left-hand side of expression (1), one obtains a value of approximately 0.2. Allowing for uncertainties in the above-mentioned parameters, it is conceivable that expression (1) could be on the verge of being satisfied.

It is, therefore, plausible that the Ingard mechanism could be responsible for the generation of the oscillations.

The author wishes to thank Dr. Uno Ingard for his helpful suggestions.

[1]J. Berlande, P. D. Goldan, and L. Goldstein, Appl. Phys. Lett. 5, 51 (1964).

[2]S. D. Strickler and A. B. Stewart, Phys. Rev. Lett. 11, 527 (1963).

[3]K. W. Gentle and U. Ingard, Appl. Phys. Lett. 5, 105 (1964).

[4]I. Alexeff and R. V. Neidigh, Phys. Rev. 129, 516 (1963).

[5]U. Ingard, Phys. Rev. 145, 41 (1966).

[6]U. Ingard and M. Schultz, Phys. Rev. 158, 106 (1967).

[7]U. Ingard and K. W. Gentle, Phys. Fluids 8, 1396 (1965).

Multiple-Mirror Confinement of Plasmas*

B. Grant Logan, A. J. Lichtenberg, M. A. Lieberman, and A. Makhijani
Department of Electrical Engineering and Computer Sciences, and the Electronics Research Laboratory, University of California, Berkeley, California 94720
(Received 14 June 1971)

Multiple-mirror confinement of high-temperature plasma for fusion application is examined by numerical techniques using a fixed-scattering-center model. It is shown, in contrast to a linear relation found in an earlier study by Post, that the confinement time increases quadratically with the number of mirrors. We present the results of this scaling on the dimensions for a multiple-mirror reactor.

In a previous communication Post[1] explored the properties of multiple-mirror systems for confining plasmas for fusion. He found that such a device, operating in a regime in which the mean free path is comparable to the system length, would have advantages over a long-mean-free-path, single-mirror device both in the scaling laws and in the suppression of velocity-space instabilities. In computer calculations, using a fixed-scattering-center model for the collisions, Post concluded that the containment time τ varied approximately linearly with the number of cells, N. However, a straightforward application of diffusion theory indicates that, provided the scattering centers are fixed, $\tau \propto L^2$, where L is the half-length of the system, independent of the mirrors. The purpose of multiple mirrors in an intermediate mean-free-path regime is to supply sufficient particle reflection at the mirrors that the self-scattering approximates scattering from fixed scattering centers, rather than free flow. Although the criteria of density and mirror ratio, for the approximation to hold, are of paramount importance for fusion reactor considerations, these criteria do not enter Post's model which assumes fixed scattering centers. It is therefore believed that Post's original calculation was not performed in the correct parameter range to determine the proper scaling of τ with system length. We therefore have performed a computer calculation similar to Post's, indicating that τ is proportional to L^2 in agreement with diffusion theory.

The charged particle is subject to two independent influences: (i) a static magnetic-mirror field in which the particle moves adiabatically, and (ii) small-angle constant scattering with the scattering center being fixed. Since the effects of the magnetic field and the collisions are considered independent, the changes in the orientation of the velocity vector of the test particle due to each are taken to be additive. The particle's position and angular velocity are advanced through small steps in which the small-angle scattering deflects the particle on a cone of half-angle α, with the azimuth on the cone selected by use of a random variable φ.

The angle α is determined from

$$\alpha^2 = \Delta\tau/\tau_\theta, \tag{1}$$

where $\Delta\tau$ is the time between steps and τ_θ is the Spitzer time,[2]

$$\tau_\theta = \frac{25.8\sqrt{\pi}\,\epsilon_0^{\,2} m^{1/2}(kT)^{3/2}}{e^4 n} \quad \text{(mks units)}, \tag{2}$$

for a deflection $\theta^2 = 1$. The numerical procedure follows that of Post,[1] except that the magnetic field is chosen either with a sinusoidal variation

$$B(z) = M^{-1}[1+\gamma\sin^2(\pi z/L)] \tag{3}$$

or similar to the more localized mirror field of Post

$$B(z) = (1+\gamma)^{-1}\{1+\gamma\exp[-\lambda\sin^2(\pi z/L)]\}, \tag{4}$$

where $\gamma = M-1$ and $M = B_{max}/B_{min}$.

Detailed calculations were performed for thermonuclear plasma parameters with two densities. The densities where chosen such that the distance l_z for scattering through an effective loss-cone angle θ_{1c} is larger than the cell length l_c at the lower density and smaller than a cell length at the higher density. l_z can be defined by

$$l_z = \bar{v}\tau_\theta\theta_{1c}^{\,2}, \tag{5}$$

with $\bar{v}$ the average axial velocity of a deuteron at energy kT and

$$\theta_{1c}^{\,2} \equiv \frac{1}{M_{eff}} \equiv 1 - \left(1 - \frac{A_{1c,\,eff}}{A_{total}}\right)^2,$$

where

$$\frac{A_{1c,\,eff}}{A_{total}} = \frac{1}{l_c}\int_0^{l_c}\left[1 - \left(\frac{B(z)}{B_{max}}\right)^{1/2}\right]dz.$$

The use of an average mirror ratio is considered to be appropriate here in that local thermalization is expected in a long system. This approximation is confirmed by numerical calculations. A temperature $kT_i = 5$ keV, a cell length $l_c = 6.5$ m, and densities, corresponding to the above criteria, of 10^{16} and 4×10^{16} were used for the calculations. Figure 1 shows a plot of the axial position of a particle versus time for $n = 4\times10^{-16}$ cm^{-3}, $M = 5$, and $N = 10$. From plots such as Fig. 1 the average distance between trapping, $\bar{l}_z$, the average trapped time $\bar{t}_1$, and the average time between trappings, $\bar{t}_2$, can be computed. These quantities are defined for a single trapping and detrapping event in Fig. 1. From the nature of the process as a random walk, the average time a particle spends in the entire system is given by

$$\tau = \bar{t}L^2/\bar{l}_z^{\,2}, \tag{6}$$

where $\bar{t} = \bar{t}_1 + \bar{t}_2$. For two configurations with the mirror ratio $M = 5$ ($M_{eff} = 1.5$), the average quantities as shown in Table I were obtained. Here

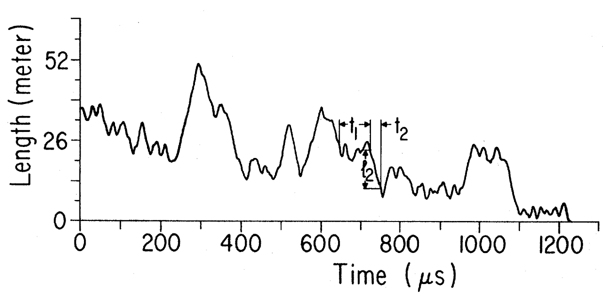

FIG. 1. Numerical plot of axial position of particle versus time; each vertical division is one mirror cell.

TABLE I. Single-particle random-walk parameters and containment times.

N	L (m)	Density (cm^3)	$\bar{t}_1$ (μsec)	$\bar{t}_2$ (μsec)	$\bar{l}_z$ (m)	τ (msec)
20	65	10^{16}	48	30	16	1.2
10	32.5	4×10^{16}	30	20	11	0.44

TABLE II. Confinement time (msec) versus peak density and number of cells.

Density (cm^{-3}) \ N	10	20	40
10^{16}	0.27	1.0	4.95
4×10^{16}	0.86	3.25	11.9

τ is calculated from Eq. (6). Averaging over the total contained time for approximately 20 particles, in each case, that are injected into a center cell of the system, we can check both the scaling law for L and the absolute value of τ as computed from Eq. (6). The average containment times for 10-, 20-, and 40-cell cases ($M=5$) were calculated in this manner and are shown in Table II. Table II confirms the approximate square-law dependence between containment time and the number of cells (length of system), in agreement with that expected from a random-walk process, or a continuity-of-flux argument.[3] The 20-cell low-density average-containment time is in good agreement with the calculated result in Table I, while the 10-cell high-density average-containment time is a factor of 2 larger than that calculated in Table I. The reason for the discrepancy in the high-density case is not fully understood, but part of the discrepancy is believed to arise from the way $\bar{t}$ and $\bar{l}_z$ are defined in Fig. 1, which considers the mirrors as the scattering units, but neglects the role of scattering centers themselves which is present in the computational model. With $M=1$ (no mirrors), the fixed scattering-center computation resulted in a contianment time approximately 25% of the containment time found above, for $M=5$.

If we assume that the plasma density in each cell is proportional to the average total time spent by a test particle in that cell, then we can construct a density profile for the multiple-mirror system. Figure 2 shows such a density profile for a 10-cell case ($M=5$). Also shown is the solution to the diffusion equation assuming a constant diffusion coefficient, a source between the fifth and sixth cells, and sinks at the ends of the multiple-mirror system. The computational asymmetry arises because the particles are injected in the center of the sixth cell rather than in the center of the system. In a device in which the primary scattering process is self-scattering, a decrease in density results in an increase of the effective diffusion coefficient since $D=\bar{l}_z^{\,2}/2\bar{t}\sim 1/nM_{\rm eff}$. In this situation the use of a constant fixed-scattering-center density is not consistent with the results of Fig. 2, unless $M_{\rm eff}$ is increased towards the mirror ends to maintain a constant D.

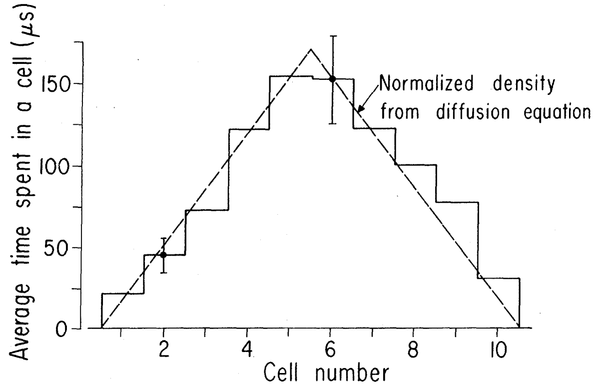

FIG. 2. Comparison of theoretical and numerical axial density distribution for constant diffusion coefficient.

The concept of local thermalization was checked by computing the ratio of the time spent in the loss cone to the total time spent in the device and comparing the ratio of the effective loss-cone phase-space area $A_{\rm 1c,eff}$ with the total phase-space area $A_{\rm total}$. The results, computed for both the sinusoidal mirrors and the more highly peaked mirrors, are presented in Table III for $M=5$. The somewhat higher values of $\tau_{\rm 1c}/\tau_{\rm total}$ found numerically, for the lower-density case, are believed due to the finiteness of the system.

The results of Table II and Fig. 2 are consistent with the calculations by Taylor[4] of the effects on a central mirror of rf stoppering. He showed that the density in the central mirror increases

TABLE III. Theoretical and numerical ratio of (time spent in loss cone)/(containment time).

$B(z)$	$A_{\rm 1c,eff}/A_{\rm total}$	Numerical $\tau_{\rm 1c}/\tau_{\rm total}$ $n=10^{16}$	$n=4\times10^{16}$
Eq. (3)	0.43	0.50	0.44
Eq. (4)	0.22	0.28	0.20

linearly with the number of rf stoppers. In our calculation the density in the central mirror also increases linearly with the number of mirror sections. However, the additional mirror sections also usefully contain particles, such that the total containment increases quadratically.

It should be emphasized that, in addition to the containment times as calculated here, there are additional considerations that bear on the usefulness of the multiple-mirror configuration as a plasma containment device. One important consideration is that, for a fully ionized plasma, the important scattering mechanism is ion-ion self-scattering in which the scattering centers have an average drift in the direction of the particle loss. These drifts due to finite loss rates have not been included in the present computational model. The drifts corresponding to the loss times reported in Tables I and II are small compared to the thermal velocity; but, nevertheless, the effect of drifts might have a serious effect on the scaling of confinement time if they were included in a self-consistent way.

A second consideration is that in some density regimes the confinement time is proportional to the density, and a fluctuation in density may cause a change in the confinement time that enhances the fluctuation. The scattering-center density distribution in the numerical model, however, is fixed.

Another important consideration is that radial losses have not been included in the numerical computations. While hydrodynamic stability may be possible without absolute minimum $\vec{B}$,[5] microinstabilities may cause radial losses in a physical system in competition to end loss.

Although additional work is required to determine the feasibility of a multiple-mirror system, it is nonetheless instructive to evaluate the computational results by estimating parameters for a D-T multiple-mirror reaction required to have a ratio (fusion thermal power generated)/(plasma kinetic energy flow) = 10. For lack of space, we report only the results: $kT_i = kT_e = 5$ keV, $n = 3 \times 10^{16}$ cm^{-3} (center), $M_{\rm eff} = 2$ (center)–13 (ends), $l_c = 6.5$ m, $L = 250$ m. The assumptions used in the reactor calculation have been previously reported.[6]

*Research sponsored by the National Science Foundation under Grant No. GK-27538, and the U. S. Air Force Office of Scientific Research under Grant No. AF-AFOSR-69-1754.

[1]R. F. Post, Phys. Rev. Lett. 18, 232 (1967).

[2]L. Spitzer, Jr., *Physics of Fully Ionized Gases* (Interscience, New York, 1956), p. 78.

[3]B. G. Logan, A. J. Lichtenberg, and M. A. Lieberman, Bull. Amer. Phys. Soc. 15, 1432 (1970).

[4]J. B. Taylor, private communication.

[5]H. P. Furth and M. N. Rosenbluth, Phys. Fluids 7, 764 (1964).

[6]B. G. Logan, Plasma Research, Electronics Research Laboratory, University of California, Berkeley, Fourth Quarterly Report, 1969 (unpublished), p. 2.

Electromagnetic Generation of Transverse Acoustic Waves in the Gigahertz Range Using Indium Films

Y. Goldstein and A. Zemel
The Racah Institute of Physics, The Hebrew University, Jerusalem, Israel
(Received 17 November 1971)

Transverse acoustic waves were generated electromagnetically at 9 GHz using In films with a conversion efficiency α of 5×10^{-5}. A good agreement is found between theory and experiment and we obtain the value of 620 Å for the superconducting penetration depth λ at $0.4T_c$ and 5×10^{10} Ω^{-1} cm^{-2} for the ratio of the conductivity to the mean free path for In. From the temperature dependence of α below the superconducting transition temperature it is concluded that pair scattering at the surface does not conserve momentum.

It was found by Abeles[1] that an electromagnetic field in the gigahertz region can generate a transverse acoustic wave at the surface of a clean indium film. Electrons in the metal are accelerated by the electromagnetic field within the penetration depth. For a thin film at low temperatures, scattering in the bulk can be neglected and the momentum gained by the electrons is transferred to the lattice by surface scattering. In the gigahertz region this momentum transfer is coherent and gives rise to a transverse acoustic wave. The theory is extremely sensitive to the